The effects of temperature and polymer composition upon the aqueous solution properties of comb-like linear poly(ethylene imine)/poly(2-ethyl-2-oxazoline) based polymers

Silvia Halacheva,[†]* Gareth J. Price[‡] and Vasil M. Garamus[§]

†*Physical and Theoretical Chemistry Laboratory, University of Oxford, South Parks Road, Oxford, OX1 3QZ, United Kingdom*

‡*Department of Chemistry, University of Bath, Claverton Down, Bath, BA2 7AY, United Kingdom*

§*Helmholtz-Zentrum Geesthacht Zentrum für Material und Küstenforschung GmbH, Max Planck Strasse 1, D-21502, Geesthacht, Germany*

Supporting information

Abstract: A range of well-defined, sparsely grafted, comb-like linear poly(ethylene imine)/poly(2-ethyl-2-oxazoline) (LPEI-comb-PEtOx) and comb-like linear poly(ethylene imine)/linear poly(ethylene imine) (LPEI-comb-LPEI) polymers with various degrees of polymerization of both main and side chains were prepared. Their aqueous solution properties were investigated by means of dynamic light scattering (DLS) and small angle neutron scattering (SANS) over a temperature range of 25 to 65 °C. For LPEI-comb-LPEI polymers the particle distributions were mono-, bi- or trimodal depending upon the temperature and/or polymer composition. The particles tended to decrease in size upon heating due to the weakening of intra- and interchain hydrogen bonds between –NH groups of the polymers and also with water

molecules. However, the aggregates formed from the LPEI-comb-LPEI polymers featuring longer main chains, shorter branches and lower grafting densities were more resistant to heat-induced disassociation. LPEI-comb-PEtOx particles featured smoother temperature variations of hydrodynamic radius and typically bimodal distributions. The shape and structure of the small LPEI-comb-PEtOx aggregates (average radius ~ 6 nm) as well as their temperature evolution were studied by SANS. A variety of structures were observed, depending upon the polymer composition. The LPEI-comb-PEtOx polymers with low grafting densities and short branches formed elongated aggregates, whereas particles of spherical core-shell structure were observed for the more densely grafted polymer with longer branches. Spherical or rod-like aggregates were monitored in LPEI-comb-LPEI aqueous solutions.

Introduction:

Stimuli-responsive materials constitute a rapidly growing field of interest in polymer and colloid science due to their ability to undergo sharp changes in their physical properties as a result of small variations in external conditions such as temperature, light, salt concentration, ionic strength and pH.[1-4] Recently, amphiphilic copolymers have attracted considerable attention because of their advantageous physical properties in the context of biomedical and nanotechnological applications such as drug delivery, cell encapsulation and tissue engineering.[5-11] When these materials are dissolved in a selective solvent, micelles of various morphologies may be formed.

Recent molecular dynamic simulations and theoretical predictions of the self-assembled structures formed from amphiphilic comb-like copolymers upon inferior solvent quality for the backbone reveal that the sequence of morphological transitions is governed by a balance between repulsive interactions among the branches and the solvophobic interactions of the main chain.[12-14] The formation of a "pearl necklace" structure, comprised of multiple spherical micelles in solution, which are stabilised by steric repulsion between coronas, has been reported for copolymers which have a sufficiently dense level of grafting. In the case of sparsely grafted copolymers, however, the formation of intramolecular aggregates of diverse morphology including pearl necklaces of spherical micelles, unimolecular wormlike cylindrical micelles and also disc-shaped, lamellar-like intramolecular aggregates were suggested.[13]

Our research is focused on the cationic polyelectrolyte poly(ethylene imine) (PEI), which has been recently recognized as one of the most efficient non-viral vectors for *in vivo* and *in vitro* transfections. At low pH, linear PEI (LPEI) is extensively protonated (at pH 2.4, ~ 70% of the amino groups are positively charged and at pH 7 this proportion decreases to 30%), whereas at high pH it is an essentially neutral polymer (at pH 10, ~ 4% are positively charged).[15-17]

Commercially available PEI is a highly branched, water-soluble polymer which is usually prepared via cationic ring-opening polymerization of ethylene imine. LPEI can be produced by the living cationic ring-opening polymerization of 2-ethyl-2-oxazoline (EtOx),[18,19] followed by alkaline or acidic hydrolysis of the resulting PEtOx.[20-24] LPEI exhibits markedly different solubility properties compared with the commercially available, highly branched PEI. Due to its linear and flexible backbone, LPEI is insoluble in water at room temperature but dissolves when heated.[24] Moreover, LPEI has been found to adopt a double-stranded helix structure in the solid-state, when free from traces of moisture.[25-28] Upon introduction of water molecules into the crystal lattice, a planar-zigzag conformation is adopted. Thermal effects upon the crystalline structure of LPEI in water have also been investigated.[29,30] The solubility change was attributed to the thermal induced conformational transition from the planar-zigzag form to random coil one, followed by hydration. In the heating/cooling cycle large hysteresis, attributed to the formation of intermolecular hydrogen bonds, has been observed. The cloud points seen in solutions of LPEI have been directly related to the polymer's melting point and the degree of polymerization.[22]

Several copolymers of other thermosensitive blocks with PEI have been explored in order to modify its cytotoxicity and transfection efficiency and their response to stimuli in solution.[31-35] Our study has focused on the solution properties of LPEI-comb-PEtOx copolymers comprised of a LPEI backbone with hydrophilic PEtOx branches. PEtOx has been identified as a biocompatible polymer, with even faster blood clearance than poly(ethylene oxide) (PEO), which makes it especially attractive for a variety of biomedical applications.[36,37] Furthermore, a cloud point temperature of around 61–64 °C, which can be tuned by varying the degree of polymerization, polymer composition and concentration, was found for PEtOx polymers with molecular weights ranging from 20 to 500 kDa.[36,38] It has also been reported that PEtOx with a molecular weight below 10 kDa does not exhibit a cloud point.[39,40]

Quantitative deacylation of LPEI-comb-PEtOx to prepare LPEI-comb-LPEI polymers has been reported.[41,42] In contrast to LPEI-comb-PEtOx, LPEI-comb-LPEI consists of insoluble branches as well as an insoluble polymer backbone (at room temperature) and to the best of our knowledge, the thermal and aqueous solution properties of these polymers remain unstudied.

Herein, we aim to quantify the physicochemical changes and possible phase-transitions of the comb-like polymers LPEI-comb-PEtOx and LPEI-comb-LPEI in water, in order to achieve a more fundamental understanding of their solution phase behaviors. The effect of the main and side chain lengths, as well as the grafting density on the aggregates formed from the various LPEI-based comb-like polymers in aqueous solution has been studied as a function of temperature using dynamic light scattering and small angle neutron scattering.

Experimental

A. Materials

All glassware was dried at 150 °C overnight and assembled under a stream of dry nitrogen. 2-Ethyl-2-oxazoline (Aldrich) was distilled from calcium hydride. Methyl *para*-toluenesulfonate (Aldrich) was purified via vacuum distillation. Acetonitrile (Aldrich, 99.8%) anhydrous, tetrahydrofuran (Aldrich, 99.9+ %, HPLC grade), anhydrous dichloromethane (Aldrich, ≥ 99.8%) and anhydrous diethyl ether (Aldrich, ≥ 99%) were used without further purification. Hydrochloric acid (32%) was purchased from Fisher Scientific. Dialysis tubing (Medicell International Ltd.,) with cutoff in the range from 3.5 to 20 kDa was used for the separation of LPEI-comb-PEtOx comb-like polymers from unreacted PEtOx. Deuterium oxide (Aldrich) and high purity water (Elga Ultrapure) were used throughout.

B. Polymerizations

Synthesis of PEtOx

The following procedure for the synthesis of $PEtOx_{66}$ is representative. 2-Ethyl-2-oxazoline (8.33 g, 84 mmol) was added to a solution of methyl *para*-toluenesulfonate (220 mg, 1.18 mmol) in 100 mL of acetonitrile, aiming to obtain PEtOx with a degree of polymerization of 71. The reaction mixture was stirred at reflux for 144 h and then cooled to room temperature. After evaporation of the solvent under reduced pressure, the residual solid was dissolved in anhydrous dichloromethane and precipitated in cold diethyl ether. After filtration, the product was dried under vacuum, yielding 7.2 g (93%) of $PEtOx_{66}$ (determined by ^1H NMR) as a yellow powder. The other $PEtOx_n$ polymers were obtained by altering the ratio of monomer (EtOx) to initiator (TsOMe).

Synthesis of LPEI

The following procedure for the synthesis of $LPEI_{96}$, is representative. $PEtOx_{96}$ (1.00 g, 0.105 mmol) was dissolved in 4.7 M $HCl_{(aq)}$ (5 mL) and heated at 100 °C for 12 h. After cooling to room temperature, the acid/water was evaporated under reduced pressure. The resulting solid was re-dissolved in water and the pH adjusted to 8–9 by addition of 2.5 M $NaOH_{(aq)}$ solution. The resulting precipitate was filtered and washed thoroughly with deionised water. The remaining water was removed by freeze-drying to afford the product as a white powder.

Synthesis of LPEI-comb-PEtOx

The following procedure for the synthesis of $LPEI_{20}$-$comb_{20}$-$PEtOx_{96}$ copolymer (the coding of samples is described below) is representative. In a separate flask, $PEtOx_{96}$ was synthesized by initiating EtOx (10.0 g, 101 mmol) with methyl *para*-toluenesulfonate (0.19 g, 1.02 mmol) in 100 mL acetonitrile. To the solution of living $PEtOx_{96}$, a hot solution of the initiator core $LPEI_{20}$ (dried by azeotropic distillation) in toluene was added. In this case, the molar ratio of oligomer

PEtOx chains to secondary amine groups (on the LPEI core) was one. The mixture was refluxed for 8 h, during which time the LPEI-comb-PEtOx formed a separate liquid phase. After cooling to room temperature, the comb-like polymer was dissolved in anhydrous dichloromethane and precipitated in cold diethyl ether. Ungrafted PEtOx oligomers were removed by dialysis (20kDa MWCO) against deionized water. Finally, water was removed from the polymer by freeze-drying.

Synthesis of LPEI-comb-LPEI

The following procedure for the synthesis of $LPEI_{20}$-$comb_{20}$-$LPEI_{96}$ is representative. The resulting $LPEI_{20}$-$comb_{20}$-$PEtOx_{96}$ copolymers were hydrolyzed by heating in 4.7 M $HCl_{(aq)}$ at 90 °C overnight. After cooling to room temperature, the pH was adjusted to 9–10 by slow addition of 2.5 M aqueous NaOH solution. The mixture was then heated to reflux under a nitrogen atmosphere and the product formed an oily layer on the surface of the solution, which became solid upon cooling. It was removed and redissolved in 600 mL of boiling water. This mixture was allowed to cool and a white suspension was obtained. After ultra centrifugation at 8000 rpm for 10 minutes, the clear liquid was decanted and the white precipitate dried via azeotropic distillation with toluene in a Dean-Stark apparatus to afford the title compound as a white solid.

C. Preparation of polymer aqueous solutions

Aqueous solutions of LPEI-comb-PEtOx were prepared by dilution of stock solutions prepared gravimetrically by adding water/D_2O to a pre-weighed quantity of the copolymer and mixing overnight under gentle mechanical agitation. LPEI-comb-LPEI and LPEI aqueous solutions were heated to 60 °C before the addition of the appropriate quantity of water/D_2O. DLS and SANS measurements were performed at polymer concentrations of 3.75 $mg.mL^{-1}$. The resulting solutions were slightly basic (pH~7.5 for LPEI-comb-PEtOx and pH ~ 9 for LPEI-comb-LPEI).

***D. Analysis**:*

Gel Permeation Chromatography (GPC)

GPC was performed using a PL-GPC50 system with tetrahydrofuran as eluent at a flow rate of 1.0 $mL.min^{-1}$. Samples were prepared as solutions in tetrahydrofuran. Calibration was performed with polystyrene standards.

Proton Nuclear Magnetic Resonance (^1H NMR)

^1H NMR spectra were recorded at 400 MHz on a Bruker ICON NMR spectrometer. The samples were prepared as solutions in $CDCl_3$ or D_2O. The chemical shifts (δ) are quoted in *ppm* and are referenced to the residual solvent peak.

Dynamic Light Scattering (DLS)

The light scattering photometer consists of a 50 mW He/Ne laser, operating at 633 nm with a standard avalanche photodiode (APD) and 90° detection optics connected to a Malvern Zetasizer Nano S90 autocorrelator. The quartz glass cylindrical cuvette was sealed and then immersed in a temperature controlled cell holder. Hydrodynamic radii (R_h) of the polymers were measured at 90°. At least 10 correlation functions were analyzed per sample, at each temperature, in order to obtain an average measurement.

Small Angle Neutron Scattering (SANS)

The SANS experiments were performed at the SANS1 instrument at the FRG1 research reactor at Helmholtz-Zentrum Geesthacht: Zentrum für Material und Küstenforschung GmbH, Geesthacht, Germany.[43] The range of scattering vectors q from 0.005 to 0.26 $Å^{-1}$ was covered by four sample-to-detector distances (from 0.7 to 9.7 m). The neutron wavelength was 8.1 Å, and the wavelength spread of the mechanical velocity selector was 10% (fwhm). The samples were kept in quartz cells (Helma, Germany) with a path length of 2 mm. For isothermal conditions, a thermostatted sample holder was used. The raw spectra were corrected for background signals

from the solvent (D_2O), sample cell, and other sources by conventional procedures. The two-dimensional isotropic scattering spectra were azimuthally averaged, converted to absolute scale, and corrected for detector efficiency by dividing by the incoherent scattering spectrum of pure water, which was measured with a 1 mm path length quartz cell. The smearing induced by the different instrumental settings was included in the data analysis.[44]

Results and discussion

Synthesis and characterization of PEtOx and LPEI polymers

The living character of the cationic ring-opening polymerization of EtOx has been extensively investigated and reviewed.[18,19,36] In this work, the strong electrophile methyl *para*-toluenesulfonate was employed to initiate the polymerization of EtOx. A number of polymerizations were carried out (Table 1) aiming to prepare polymers with degrees of polymerization (DPs) from 20 to 99.

The PEtOx polymers were characterized by GPC and ^{1}H NMR. The polymer characterization data are shown in the Supporting Information. GPC analyses gave monomodal distributions with dispersity indices ranging from 1.1 to 1.3. The DPs of the PEtOx were estimated from the ^{1}H NMR spectra of the polymers in $CDCl_3$. The experimental DPs are in good agreement with the theoretical values and with those calculated from the feed (Table 1).

LPEI was obtained by acidic hydrolysis of PEtOx. It was reported previously that the degree of deacylation of PEtOx could be controlled by the amount of acid used.[21] To facilitate the complete hydrolysis, an excess of acid was employed. Examination of the ^{1}H NMR spectra revealed the degree of hydrolysis to be >95%. The DP of the resulting LPEI was confirmed as equivalent to that of the corresponding PEtOx precursors (see Supporting Information).

PEtOx					LPEI		
DP		Dispersity by GPC	M_n[a]	Code	DP[b]	M_n[b]	Code
Theor.	Exp.[a]						
20	20	1.1	2000	$PEtOx_{20}$	20	860	$LPEI_{20}$
50	48	1.2	4800	$PEtOx_{48}$	48	2100	$LPEI_{48}$
71	66	1.3	6600	$PEtOx_{66}$	66	2900	$LPEI_{66}$
99	96	1.2	9600	$PEtOx_{96}$	96	4200	$LPEI_{96}$

Table 1. Characterization data for PEtOx and LPEI polymers.

[a] Determined by ^{1}H NMR ($CDCl_3$);

[b] Determined by ^{1}H NMR (D_2O, 60 °C).

Synthesis of LPEI-comb-PEtOx and LPEI-comb-LPEI polymers.

The LPEI-comb-PEtOx and LPEI-comb-LPEIs were synthesized by a comb-burst branching strategy, as utilized by Tomalia.[41,42] Recently, this method has been successfully applied by Aoi[45] to obtain chitin derivatives featuring PEtOx side chains. The technique involves the grafting of PEtOx chains onto a LPEI "initiator core" in order to produce comb-branched LPEI-comb-PEtOx copolymers. These compounds were then hydrolysed in order to obtain the final LPEI-comb-LPEI products. In particular, the reaction involves the quenching of the living PEtOx oligomers onto secondary amines of LPEI resulting in LPEI-comb-PEtOx in good yields (Figure 1). This strategy allows a significant control of the critical molecular design parameters, such as size, shape, surface chemistry and topology. For example, when the blocks of LPEI are particularly long, rod-type morphology can be expected, whereas spherical forms are favored when the blocks

are shorter. A number of polymerizations were carried out, aiming to prepare sparsely grafted comb-like polymers with random graft positions and with varying chain lengths of both LPEI backbone and PEtOx branches. The polymer compositions and degrees of grafting (DG) were determined from the ^{1}H NMR spectra in D_2O (see Supporting Information). This data is presented in Table 2. All comb-like polymers have also been characterized by solid-state Fourier Transform Infrared (FTIR) spectroscopy. The transmittance FTIR spectra of some of the solid LPEI-comb-PEtOx and LPEI-comb-LPEI polymers are shown elsewhere.[46] The structure of LPEI-comb-PEtOx and the final LPEI-comb-LPEI polymers is schematically presented in Figure 2.

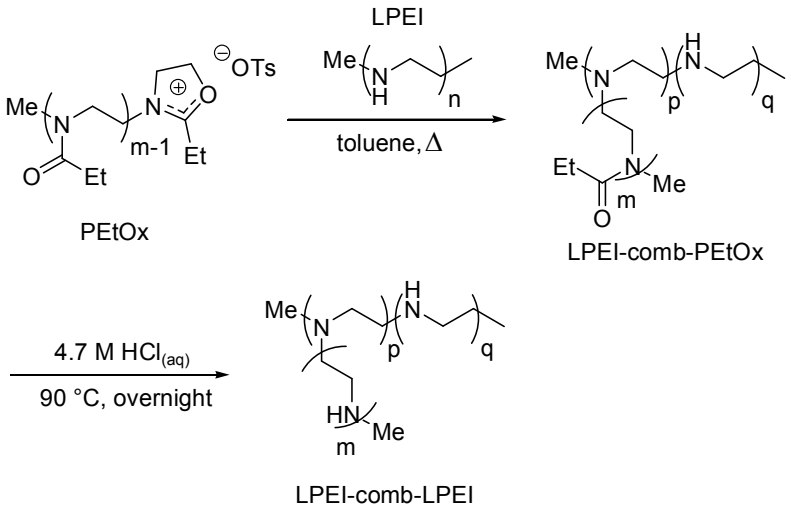

Figure 1. Synthesis of LPEI-comb-PEtOx and LPEI-comb-LPEI polymers (where p + q = n).

DP of main chain ($LPEI_n$)[a]	*DP of branches ($PEtOx_n$)*[a]	*DG*[b]	*LPEI content in LPEI-comb-PEtOx (mol %)*	*Code LPEI-comb-PEtOx*	*Code LPEI-comb-LPEI*
66	48	4%	34	$LPEI_{66}$-$comb_4$-$PEtOx_{48}$	$LPEI_{66}$-$comb_4$-$LPEI_{48}$
96	48	5%	29	$LPEI_{96}$-$comb_5$-$PEtOx_{48}$	$LPEI_{96}$-$comb_5$-$LPEI_{48}$
66	66	7%	18	$LPEI_{66}$-$comb_7$-$PEtOx_{66}$	$LPEI_{66}$-$comb_7$-$LPEI_{66}$
20	96	20%	5	$LPEI_{20}$-$comb_{20}$-$PEtOx_{96}$	$LPEI_{20}$-$comb_{20}$-$LPEI_{96}$

Table 2. Characterization data for LPEI-comb-PEtOx and LPEI-comb-LPEI polymers.

[a] Determined from ^{1}H NMR spectra of PEtOx and LPEI precursors (see Table 1);

[b] Determined from ^{1}H NMR spectra of LPEI-comb-PEtOx in D_2O at 60 °C; the data is in agreement with that previously reported.[32,47]

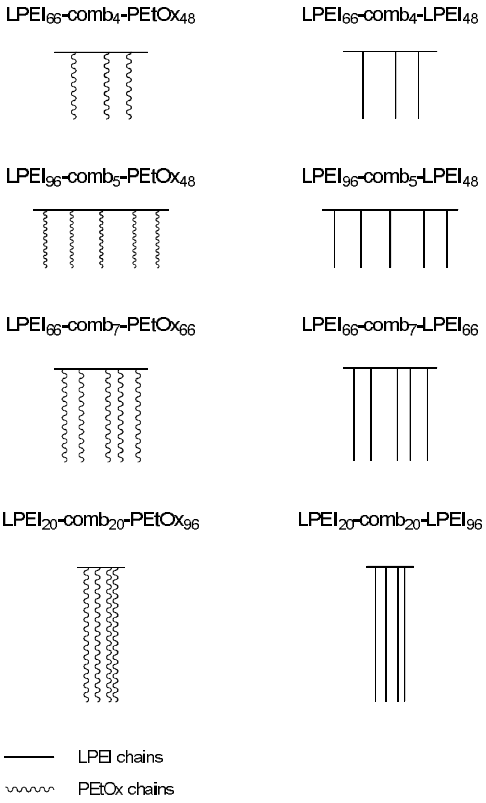

Figure 2. Representation of polymer structures. The structures are not intended to reflect the polymer's conformation in solution.

Dynamic Light Scattering

In this section we consider the solution properties of sparsely grafted LPEI-comb-PEtOx and LPEI-comb-LPEI copolymers in water. For comparison purposes, the solution behavior of the related LPEI polymers was studied as well. For LPEI-comb-PEtOx, water is a poor solvent for the main chain at ambient temperatures but efficiently solvates the branches. Solutions of LPEI-comb-PEtOx appeared optically transparent at all temperatures. They remained stable and clear for at least one month after preparation. LPEI and LPEI-comb-LPEI were initially dissolved by heating the solutions to 60 °C, followed by cooling to 45 °C. The solutions were equilibrated at 45 °C for 15 min and then quickly placed into the DLS holder. The solutions appeared

moderately to highly opalescent and only became clear at the highest temperatures tested. DLS measurements were carried out at five different temperatures (25, 35, 45, 55, and 65 °C) for the LPEI-comb-PEtOx polymers and at 45, 55 and 65 °C for LPEI and LPEI-comb-LPEI polymers. The observation of bi- or trimodal relaxation time distributions made the determination of the static light scattering parameters impossible.

Examples of relaxation time distributions for LPEI, LPEI-comb-PEtOx and LPEI-comb-LPEI polymers are shown in Figure 3. The calculated hydrodynamic radii are summarized in Table 3. For LPEI, at 45 °C, along with the fast modes corresponding to particles with dimensions of several nm, slow modes of amplitude ≥ 47% and R_h^{slow} ≥ 155 nm were also observed. Upon increasing the temperature, however, the slow modes disappeared and distribution was monomodal (see Figure 3a). For both $LPEI_{66}$-$comb_4$-$LPEI_{48}$ and $LPEI_{96}$-$comb_5$-$LPEI_{48}$ the distributions were monomodal at all temperatures tested. At 45 °C large particles with radii of 407 nm and 899 nm were observed for the solutions of $LPEI_{66}$-$comb_4$-$LPEI_{48}$ and $LPEI_{96}$-$comb_5$-$LPEI_{48}$, respectively, which decreased to 52 nm and 114 nm upon heating to 65 °C. For the other LPEI-comb-LPEI polymers accompanying modes were observed at elevated temperatures (see Figure 3b). Typically, the slow modes featured amplitudes of ≥ 62% and correspond to particles with dimensions from 82 to 480 nm. Fast particles with R_h^{fast} ≤ 32 nm and amplitudes ≤ 6% were responsible for intermediate modes observable at 55 °C. Of particular interest are the fast modes which appeared upon heating the solutions of $LPEI_{20}$ to 55–65 °C. These particles have radii of several nm and it is reasonable to assume that they are unimers. The dissolution of LPEI in water upon heating has been recently described in terms of melting of the hydrated polymer crystals.[22,30] Furthermore, the latest simulation data described the conformation of a linear polymer under poor solvent conditions as a globule of densely packed blobs which unfold in the presence of a good solvent.[48,49] By the use of DLS we are now able to directly monitor the

thermal effect upon the LPEI and LPEI-comb-LPEI particles in solution and determine the factors which affect the aggregates' stabilities. The data show that upon heating, the large particles gradually dissociated into smaller aggregates, their contribution to the scattering light decreases and eventually the polymers dissolve to unimers. This can be attributed to the weakening of intra- and interchain hydrogen bonds between water and the –NH groups of LPEI[29,30,50] and LPEI-comb-LPEI, leading to an increase in the polymer mobility and solubility. Recently, disintegration of large micron-size aggregates upon heating has been also reported for the poly(glycidol)-based analogues to the *Pluronic*® block copolymers.[51,52] The disintegration of the large particles has been assigned to the breakdown of the multiple intra- and interchain hydrogen bonds in the poly(glycidol) moieties, either via direct poly(glycidol)-poly(glycidol) interactions or interactions mediated through water molecules. In contrast to $LPEI_{96}$, where the slow particles are still observed at 55 °C, the aggregates formed from $LPEI_{20}$ dissolved at this temperature. This is not surprising, as LPEI crystals of lower molecular weights are known to possess correspondingly lower dissolution temperatures in aqueous solution.[22] Compared to the LPEI, LPEI-comb-LPEI aggregates do not completely dissociate, with the small particles either accompanied by their larger counterparts or else not observed in the solution at all. The most resistant to heat-induced dissociation are the particles formed of LPEI-comb-LPEI polymers with longer main chain, shorter branches and lower grafting density ($LPEI_{96}$-$comb_5$-$LPEI_{48}$ and $LPEI_{66}$-$comb_4$-$LPEI_{48}$). Although these particles reduce significantly their size upon heating, at elevated temperatures the relaxation time distribution were still monomodal, evidencing the existence of large object with dimension over 50 nm. However, under the same conditions, the aggregates formed from the remaining two LPEI-comb-LPEI polymers – $LPEI_{66}$-$comb_7$-$LPEI_{66}$ and $LPEI_{20}$-$comb_{20}$-$LPEI_{96}$ – were found to decrease in size to particles with radii of just a few nanometers. The initial temperature increase, from 45 to 55 °C, was found to reduce a larger

proportion of the $LPEI_{20}$-$comb_{20}$-$LPEI_{96}$ aggregates to significantly smaller particles in comparison with the $LPEI_{66}$-$comb_{7}$-$LPEI_{66}$ aggregates. Moreover at 65 °C the larger slow particles were observed in $LPEI_{66}$-$comb_{7}$-$LPEI_{66}$ aqueous solutions. The data clearly shows that the important factors influencing the thermal resistance of the polymer particles are the length of the main chain and branches, as well as the grafting density. The particles' size and thermal stability over the entire temperature range was found to decrease in the following order: $LPEI_{96}$-$comb_{5}$-$LPEI_{48}$ > $LPEI_{66}$-$comb_{4}$-$LPEI_{48}$ > $LPEI_{66}$-$comb_{7}$-$LPEI_{66}$ >$LPEI_{20}$-$comb_{20}$-$LPEI_{96}$.

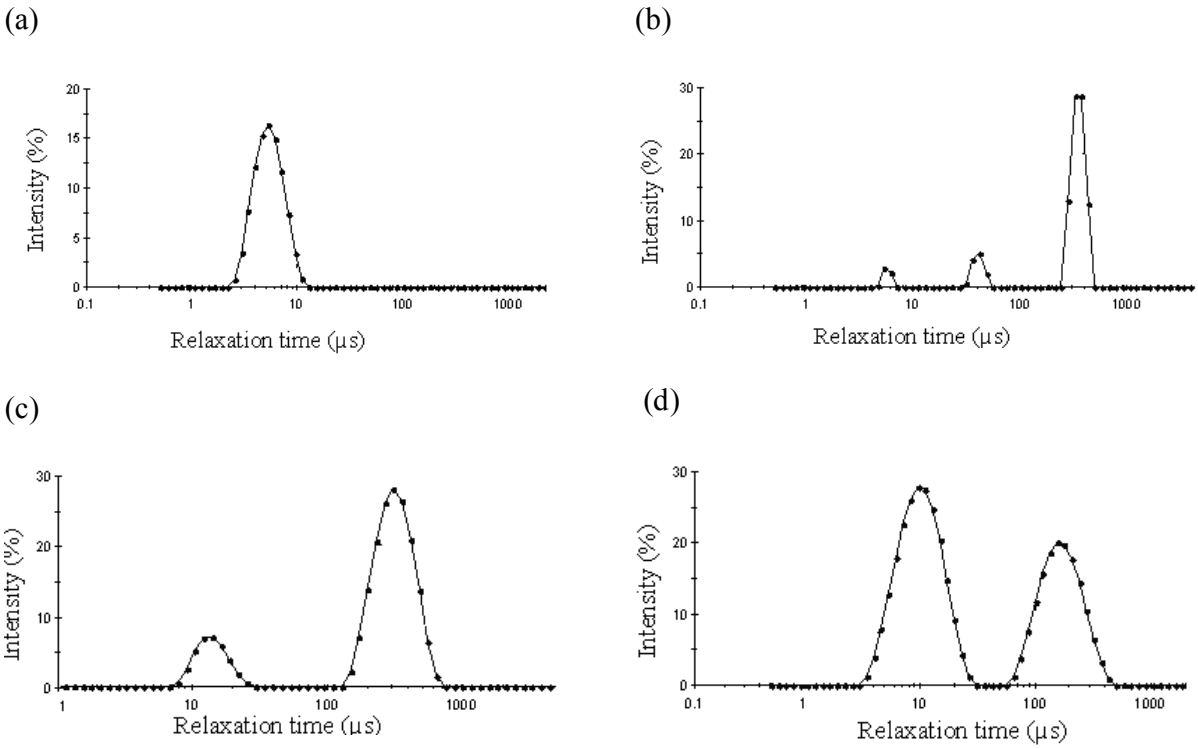

Figure 3. Relaxation time distributions for 3.75 $mg.mL^{-1}$ aqueous solutions of: (a) $LPEI_{96}$ at 65 °C; (b) $LPEI_{66}$-$comb_{7}$-$LPEI_{66}$ at 55 °C ; (c) $LPEI_{66}$-$comb_{4}$-$PEtOx_{48}$ at 25 °C; (d) $LPEI_{66}$-$comb_{7}$-$PEtOx_{66}$ at 65 °C.

T (°C)	25[a]	35[a]	45	55	65
Polymer					
$LPEI_{20}$	-	-	b $^{47}155$; $^{53}5.1$	0.8	0.8
$LPEI_{96}$	-	-	b $^{90}329$; $^{10}5.1$	b $^{36}220$; $^{64}4.4$	4.4
$LPEI_{20}$-$comb_{20}$-$LPEI_{96}$	-	-	247	c $^{80}141$; $^{3}14$; $^{17}3.9$	b $^{80}82$; $^{20}3.5$
$LPEI_{66}$-$comb_{7}$-$LPEI_{66}$	-	-	b $^{91}480$; $^{9}48$	c $^{83}277$; $^{6}32$; $^{11}4.5$	b $^{62}104$; $^{38}3.4$
$LPEI_{66}$-$comb_{4}$-$LPEI_{48}$	-	-	407	247	52
$LPEI_{96}$-$comb_{5}$-$LPEI_{48}$	-	-	899	669	114
$LPEI_{20}$-$comb_{20}$-$PEtOx_{96}$	b $^{40}128$; $^{60}7.3$	b $^{42}144$; $^{58}6.3$	b $^{48}115$; $^{52}6.4$	b $^{47}131$; $^{53}6.3$	b $^{45}104$; $^{55}6.2$
$LPEI_{66}$-$comb_{7}$-$PEtOx_{66}$	b $^{37}156$; $^{63}12$	b $^{29}132$; $^{71}11$	b $^{27}142$; $^{73}10$	b $^{32}135$; $^{68}9.1$	b $^{40}140$; $^{60}8.9$
$LPEI_{66}$-$comb_{4}$-$PEtOx_{48}$	b $^{57}110$; $^{43}4.9$	b $^{55}114$; $^{45}4.9$	b $^{53}127$; $^{47}4.7$	b $^{55}124$; $^{55}4.7$	b $^{55}99$; $^{55}4.3$
$LPEI_{96}$-$comb_{5}$-$PEtOx_{48}$	b	b	b	b	b

	$^{58}122$; $^{42}7.3$	$^{55}113$; $^{45}7.2$	$^{53}148$; $^{47}7.3$	$^{49}97$; $^{51}6.6$	$^{49}87$; $^{51}6.4$

Table 3. Variation of the hydrodynamic radius (R_h)[d] in nm with temperature for LPEI, LPEI-comb-LPEI and LPEI-comb-PEtOx polymers in aqueous solution.

[a] No measurements were performed for LPEI and LPEI-comb-LPEI at temperatures of 25 and 35 °C.

[b] Bimodal distribution

[c] Trimodal distribution

[d] The intensities of the different modes as percentages are presented as superscript on the particles R_h .

In contrast to LPEI and LPEI-comb-LPEI, LPEI-comb-PEtOx polymers formed smaller particles in aqueous solution, with smoother temperature variations of R_h^{slow}. The relaxation time distributions were typically bimodal at all temperatures (see Figure 3c–d). The particles responsible for the slow modes are with R_h^{slow} from 87 to 156 nm. The fast modes are with amplitudes approximately equal to or higher than those of the slow modes at elevated temperatures and correspond to particles which cover the R_h^{fast} range from 4.3 to 12.0 nm (see Table 3). It is reasonable to assume that these are dimers, trimers or slightly larger aggregates, which also appear to be dominant particles in solutions. For all samples, a decrease in R_h^{slow} was observed with increasing temperature, a feature which correlates well with the increasing solubility of LPEI moieties upon heating. The addition of PEtOx side chains and the accompanying change in macromolecular topology had a dramatic effect on the solubility of the polymer as a whole. Despite the collapse LPEI backbone at room temperature, the copolymer

solutions are stable with respect to microphase separation. The temperature sensitivity of thermosensitive polymers depends upon the extent of the interactions of polymer segments with water via hydrogen bonding. Increasing the temperature weakens the hydrogen bonds between polymer and water molecules, and depending on the hydrophilic/hydrophobic balance of the polymers a macroscopically observable precipitation at well defined Low Critical Solution Temperature (LCST) can be observed.[53,54] Recently, Weber[40] has studied the aqueous solution behavior of comb-like copolymers with hydrophilic oligo(2-ethyl-2-oxazoline) side chains and hydrophobic methacrylate backbones. By incorporating sufficiently low molecular weight PEtOx (which does not feature an LCST) moieties onto a methacrylate backbone, they obtained PEtOx-based comb-like polymers which exhibit the LCST behavior of high molecular weight PEtOx. Tuning of the cloud point (CP) by varying molecular weight and composition for other PEtOx-based copolymers has also been achieved.[36,39] LPEI-comb-PEtOx polymers do not cloud within the temperature range studied. However, significant dehydration of the PEtOx block is expected at high temperatures.

Comparing the results for the copolymer with the highest ($LPEI_{96}$-$comb_5$-$PEtOx_{48}$) and the lowest ($LPEI_{20}$-$comb_{20}$-$PEtOx_{96}$) LPEI contents, the larger decrease in R_h^{slow} upon heating was observed for the former polymer (from 122 nm at 25 °C to 87 nm at 65 °C). A similar trend was previously reported for aqueous solutions of poly(*p*-dioxanone)-grafted-poly(vinyl alcohol) upon heating, where a transition from LCST to Upper Critical Solution Temperature (UCST) phase behavior was observed by varying the hydrophobic/hydrophilic balance of the copolymer.[55] In order to investigate the particle structure and possible phase transitions induced by changing solvent strength and how these are affected by the polymer composition, aqueous solutions of the comb-like LPEI-based copolymers were further studied by SANS and the results are shown below.

SANS analysis:

SANS experiments were performed at 25, 45 and 60 °C for LPEI-comb-PEtOx and 45 °C for some of the LPEI-comb-LPEI polymers.

Representative SANS profiles for selected LPEI-comb-PEtOx polymers are shown in Figure 4. The scattering data were first analyzed by slope determination (i.e., $I(q) \sim q^{-\alpha}$). The slopes at different q ranges were calculated and selected examples are presented in Table 4. As seen in Figure 4, the scattering curves of the polymers are similar in shape and at low q range ($q < 0.03$ Å^{-1}) the scattering from structures with an average radius of 60 Å could be detected. On the q scale of the SANS measurements no traces of scattering from the large LPEI-comb-PEtOx particles (seen as a slow mode by DLS) were observed. Therefore, it has been assumed that the main scattering objects in the SANS experiments are the small particles, which were detected as a fast mode by DLS.

The complete q range was analyzed by the Indirect Fourier Transformation (IFT) approach developed by Glatter[56] and later revised by Pedersen.[57] Details of this analysis are presented in the Supporting Information. This approach requires only limited information on the possible shapes of the aggregates: sphere-like (all three dimensions are of same length scale), rod-like (one size-dimension is much larger than the other two) or sheet-like (one dimension is small relative to the other two). Previously, IFT has been successfully applied to characterize aqueous solution properties of a range of polymer and surfactant systems.[51,58,59]

Application of IFT enabled us to calculate the shape of the $p(r)$ function (pair distance distribution function); from the $p(r)$ function it is possible to calculate: $I(0)$ (scattering at "zero angle") and R_g (radius of gyration of neutron scattering contrast within the aggregate). The values of these two quantities for each polymer are shown in Table 4. At elevated temperatures the

scattering contrast of the particles becomes larger (i.e., $I(0)$ increases and R_g decreases upon heating) which could be attributed to polymer dehydration.

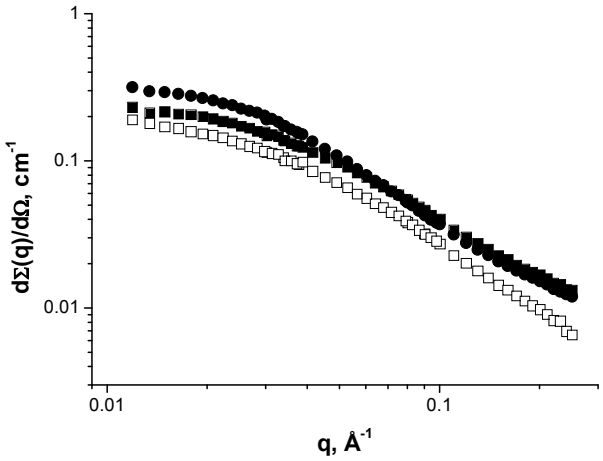

Figure 4. SANS profiles obtained from 3.75 mg.mL^{-1} aqueous dispersions of LPEI$_{96}$-comb$_5$-PEtOx$_{48}$ (open squares) at 25 °C; LPEI$_{96}$-comb$_5$-PEtOx$_{48}$ (closed squares) and LPEI$_{66}$-comb$_7$-PEtOx$_{66}$ (closed circle) at 60 °C.

Polymer	T	Slopes at q ranges		D_{max}	$I(0)$, (cm^{-1})	R_g	r
	°C	0.01-0.03	0.1-0.3	$D_{max,CS}$	$I_{CS}(0)$, (cm^{-1}nm^{-1})	$R_{CS,g}$	r_{CS}
				(nm)		(nm)	(nm)
	25	0.61	0.73	15	0.080±0.002	4.76±0.13	6.2
LPEI$_{20}$-comb$_{20}$-PEtOx$_{96}$	45	0.60	0.85	15	0.083±0.004	4.65±0.1	6.0
	60	0.53	0.63	15	0.090±0.002	4.46±0.13	5.8
	25	0.56	1.54	15	0.185±0.002	4.40±0.06	5.7
				3.5	0.011±0.0001	1.15±0.02	1.62
	45	0.54	0.83	15	0.206±0.003	4.41±0.07	5.7
LPEI$_{96}$-comb$_5$-PEtOx$_{48}$				3.5	0.013±0.0001	1.13±0.02	1.58

	60	0.46	0.69	13	0.209±0.005	3.86±0.06	5.0
				4	0.014±0.0001	1.08±0.02	1.5
	25	0.60	1.55	15	0.244±0.004	4.62±0.05	6.0
				6	0.014±0.0001	1.57±0.03	2.2
	45	0.60	1.24	15	0.278±0.003	4.59±0.05	5.9
$LPEI_{66}$-$comb_{7}$-$PEtOx_{66}$				6	0.016±0.0001	1.55±0.02	2.17
	60	0.49	1.83	15	0.328±0.004	4.54±0.06	5.9
				6	0.019±0.0001	1.57±0.03	2.2
	25	0.64	1.55	17	0.189±0.004	4.76±0.13	6.1
				3.5	0.011±0.0001	1.06±0.02	1.49
	45	0.60	1.19	17	0.215±0.003	4.74±0.13	6.1
$LPEI_{66}$-$comb_{4}$-$PEtOx_{48}$				3.5	0.014±0.0001	1.07±0.02	1.50
	60	0.55	0.82	15	0.212±0.005	4.01±0.1	5.2
				3.5	0.015±0.0001	1.03±0.02	1.45

Table 4. SANS data of the particles formed from LPEI-comb-PEtOx polymers in aqueous solutions. Slopes of $I(q) \sim q^{-\alpha}$ plots at different q ranges; scattering at "zero angle" $I(0)$ or cross sectional scattering at zero angle, $I_{CS}(0)$; radius of gyration (R_g) or cross sectional radius of gyration ($R_{CS,g}$); finite maximum dimensions of the small particles (D_{max}); equivalent sphere radius r or equivalent radius of circular cross section r_{CS} of the aggregates.

$LPEI_{20}$-$comb_{20}$-$PEtOx_{96}$. The scattering curves were analyzed using the IFT model, assuming sphere-like geometry. Figure 5 shows the evolution of the $p(r)$ function with temperature for the solution of $LPEI_{20}$-$comb_{20}$-$PEtOx_{96}$. The $p(r)$ function is highly asymmetric and displays more

than one maximum value within the temperature range tested. The first maximum was attributed to the compact LPEI domains, whereas the second can be attributed to scattering from the corona (presumably consisting of PEtOx branches) which becomes more compact as the temperature increases. The third maximum in $p(r)$ function may be related to the maximum size of the particles, which is ~10 nm (R_h^{fast} ~6 nm, see DLS). Although increasing the temperature did not cause significant alterations in the aggregates' structures, a slight decrease in the total size of the aggregates and a more pronounced level of scattering from their interior was observed.

The R_g values were determined from the second moment of the $p(r)$ functions (Table 4) and are related to both the size of the particles and the distribution of the scattering length density within the particles (see Supporting Information). For homogeneous objects, radii of equivalent spheres, r, could be calculated from R_g, where $r = (5/3)^{1/2}R_g$. For all LPEI-comb-PEtOx polymers the values of r are slightly smaller than those of R_h^{fast}, as determined by DLS. This is probably due to the presence of a hydration layer which gives a significant contribution to the DLS results but is almost invisible by SANS.

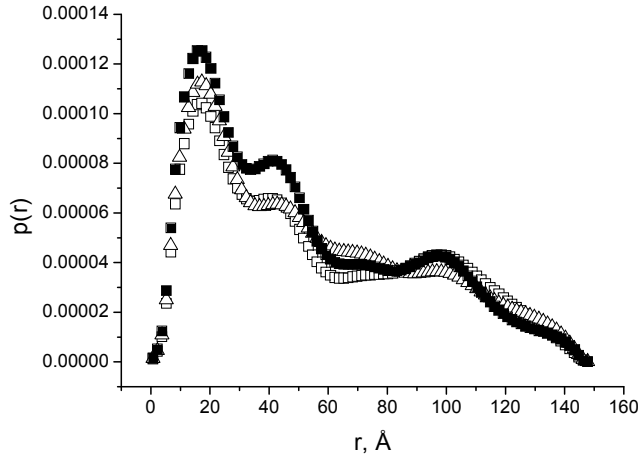

Figure 5. Pair distance distribution function, $p(r)$, obtained from the SANS data of a 3.75 mg.mL^{-1} solution of $LPEI_{20}$-$comb_{20}$-$PEtOx_{96}$ at 25 °C (open squares), 45 °C (open triangles) and 60 °C (closed squares).

$LPEI_{96}$-$comb_5$-$PEtOx_{48}$. The scattering data for $LPEI_{96}$-$comb_5$-$PEtOx_{48}$, the polymer with the longest LPEI backbone, was analyzed according to the IFT model, assuming sphere-like and rod-like geometries. Figure 6a shows the evolution of $p(r)$ function with temperature. At all temperatures, the $p(r)$ function is asymmetric; it decreases gradually at long distances, which implies that the aggregates are anisotropic, presumably rod-like. The scattering intensity for rod-like aggregates can be expressed via a cross section pair-distance distribution function $p_{cs}(r)$ (see Figure 6b). Its Gaussian shape is characteristic for almost homogeneous, cylindrical crew-cut aggregates. It is reasonable to assume that they are composed of a cylindrical LPEI core surrounded by a thin PEtOx corona. Compared with $LPEI_{20}$-$comb_{20}$-$PEtOx_{96}$, the R_g values for $LPEI_{96}$-$comb_5$-$PEtOx_{20}$ are somewhat smaller (see Table 4). One possible explanation is the higher contribution of the PEtOx side chains to the scattering for $LPEI_{20}$-$comb_{20}$-$PEtOx_{96}$, relative to that of $LPEI_{96}$-$comb_5$-$PEtOx_{48}$.

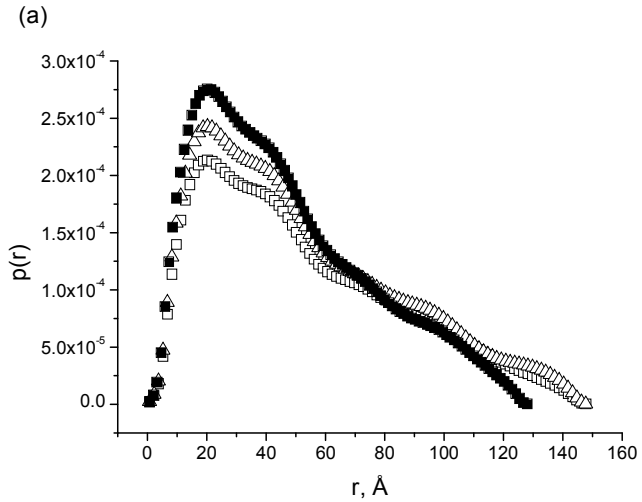

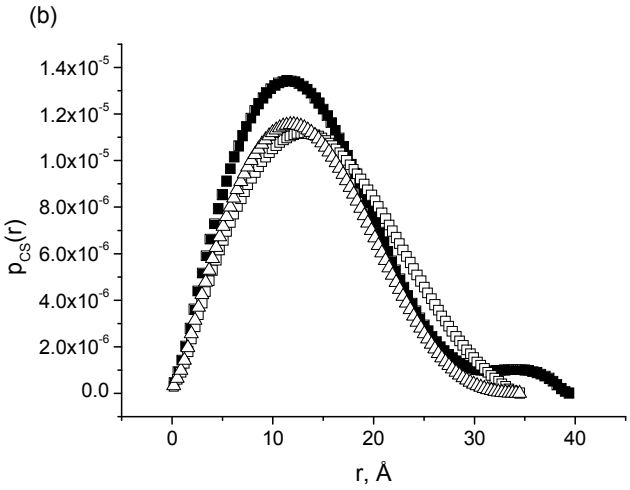

Figure 6. (a) Pair distance distribution function, $p(r)$ and (b) cross section pair distance distribution function, $p_{CS}(r)$ for a 3.75 mg.mL^{-1} solution of LPEI$_{96}$-comb$_5$-PEtOx$_{48}$ at 25 °C (open squares), 45 °C (open triangles) and 60 °C (closed squares).

LPEI$_{66}$-comb$_4$-PEtOx$_{48}$ and LPEI$_{66}$-comb$_7$-PEtOx$_{66}$. The aqueous solution behaviors of these polymers are very similar to that observed for LPEI$_{96}$-comb$_5$-PEtOx$_{48}$. At all temperatures, the asymmetric shapes of the $p(r)$ functions for LPEI$_{66}$-comb$_4$-PEtOx$_{48}$ (see Supporting Information) and LPEI$_{66}$-comb$_7$-PEtOx$_{66}$ (Figure 7a) point to an anisotropic shape of the aggregates. Slight decreases in the particle dimensions were observed for LPEI$_{66}$-comb$_4$-PEtOx$_{48}$ at elevated temperatures, when the contribution of the core to the overall scattering of the aggregates is increased (Table 4). A further reanalysis by IFT as scattering from rod-like particles gave the p_{CS}(r) functions shown in Figure 7b and in the Supporting Information. The shape of the $p_{CS}(r)$ function for LPEI$_{66}$-comb$_4$-PEtOx$_{48}$ is only slightly asymmetric, with a decrease of both cross-section size and asymmetry at high temperatures, suggesting that the cylindrical cross-sections of LPEI$_{66}$-comb$_4$-PEtOx$_{48}$ aggregates become more compact and closer to circular (see Supporting Information). The $p_{CS}(r)$ function for LPEI$_{66}$-comb$_7$-PEtOx$_{66}$ aggregates exhibits two maxima

which can be explained by the core-shell model (Figure 7b). The analysis implies that the cylindrical structures consist of a core and shell (the contribution of the shell increases with temperature) and do not exhibit detectable changes in size over the temperature range studied (see Table 4).

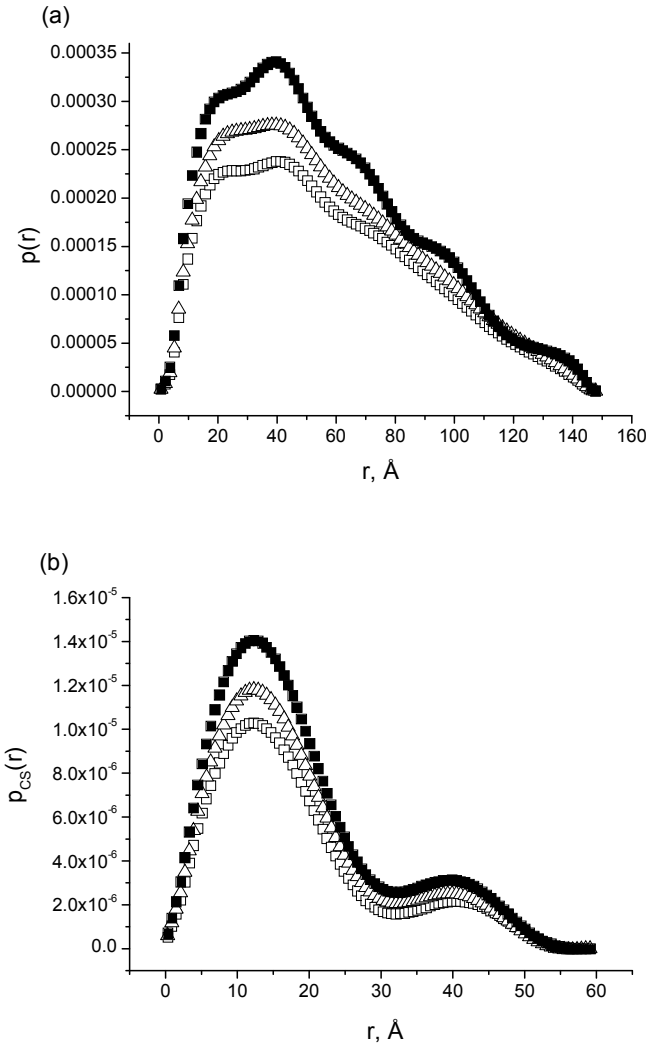

Figure 7. (a) Pair distance distribution function, $p(r)$, and (b) cross-section pair distance distribution function, $p_{CS}(r)$ for 3.75 mg.mL^{-1} solutions of LPEI$_{66}$-comb$_7$-PEtOx$_{66}$ at 25 °C (open squares), 45 °C (open triangles) and 60 °C (closed squares).

LPEI-comb-LPEI polymers. The $p(r)$ distribution functions for $LPEI_{66}$-$comb_7$-$LPEI_{66}$ and $LPEI_{96}$-$comb_5$-$LPEI_{48}$ at 45 °C are shown in Figure 8a. For $LPEI_{66}$-$comb_7$-$LPEI_{66}$ the corresponding $p(r)$ function is characterized by two maxima at short and long distances, which are attributed to the scattering of the main chain and of the branches, respectively. The particles formed are large, with radii of over 100 Å. The data correlate well with the particle dimensions indicated by DLS. The largest particles are these formed from $LPEI_{96}$-$comb_5$-$LPEI_{48}$. The almost-Gaussian shape of the $p(r)$ function for this polymer implies that the particles are compact and close to spherical. The data for $LPEI_{66}$-$comb_7$-$LPEI_{66}$ showed values of slopes at low q close to -1 which is characteristic of rod-like objects. IFT analysis for rod-like objects adequately accounted for the data with the $p_{CS}(r)$ function shown in Figure 8b. Its asymmetric shape is indicative of an elliptical cross-section for $LPEI_{66}$-$comb_7$-$LPEI_{66}$ aggregates.

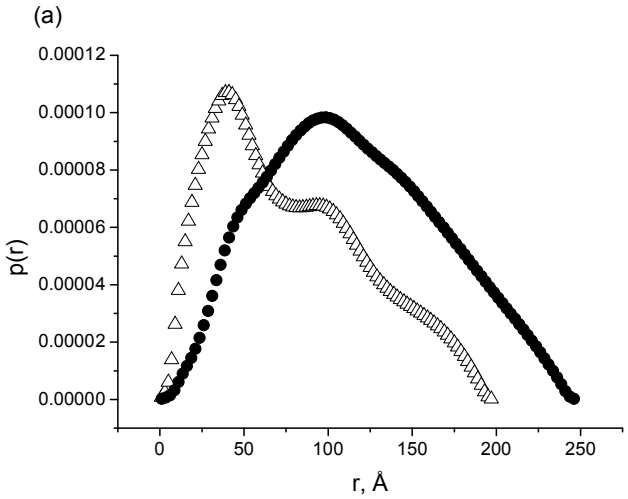

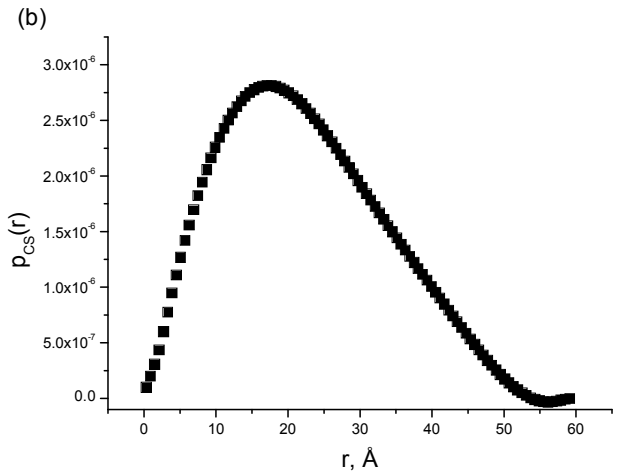

Figure 8. (a) Pair distance distribution function, $p(r)$ for 3.75 mg.mL^{-1} solutions of LPEI$_{66}$-comb$_7$-LPEI$_{66}$ (open triangles) and LPEI$_{96}$-comb$_5$-LPEI$_{48}$ (closed ovals) at 45 °C; (b) cross-section pair distance distribution function, $p_{CS}(r)$ for a 3.75 mg.mL^{-1} solution of LPEI$_{66}$-comb$_7$-LPEI$_{66}$ at 45 °C.

Concluding remarks

A range of LPEI and sparsely grafted, random LPEI-comb-PEtOx and LPEI-comb-LPEI polymers have been synthesized and their aqueous solution-phase behaviors studied over a range of temperatures. Large particles which tended to decrease in size upon heating were observed in both the LPEI and LPEI-comb-LPEI solutions. In contrast to LPEI, the formation of larger and more thermally stable particles was observed in the LPEI-comb-LPEI aqueous solutions. The thermal stability was more pronounced for the polymers featuring longer backbones, shorter branches and lower grafting densities (LPEI$_{96}$-comb$_5$-LPEI$_{48}$ and LPEI$_{68}$-comb$_4$-LPEI$_{48}$). LPEI-comb-PEtOx polymers were found to form smaller aggregates with smoother temperature variations of R_h. The shape and internal structure of the LPEI-comb-PEtOx and LPEI-comb-LPEI aggregates, as well as the temperature evolution of LPEI-comb-PEtOx particles was further

studied by SANS. The LPEI-comb-PEtOx particles (observable as fast modes by DLS) were composed of compact LPEI domains, with PEtOx corona. They also exhibit structural polymorphism, which depends upon the polymer composition. The polymers with low grafting density and short branches form aggregates of anisotropic, rod-like shape ($LPEI_{96}$-$comb_5$-$PEtOx_{48}$, $LPEI_{66}$-$comb_4$-$PEtOx_{48}$, $LPEI_{66}$-$comb_7$-$PEtOx_{66}$), whereas particles featuring a spherical core-shell structure were observed when the polymer was densely grafted, with long branches ($LPEI_{20}$-$comb_{20}$-$PEtOx_{96}$, see Figure 9). For $LPEI_{66}$-$comb_4$-$PEtOx_{48}$ aggregates, an increase in temperature led to formation of cylindrical aggregates with more compact, nearly circular cross-sections. Core-corona type cylindrical aggregates were observed for $LPEI_{66}$-$comb_7$-$PEtOx_{66}$ aqueous solutions. In contrast to $LPEI_{66}$-$comb_7$-$LPEI_{66}$, where the scattering data were described by assuming rod-like geometry, $LPEI_{96}$-$comb_5$-$LPEI_{48}$ formed compact and almost spherical aggregates.

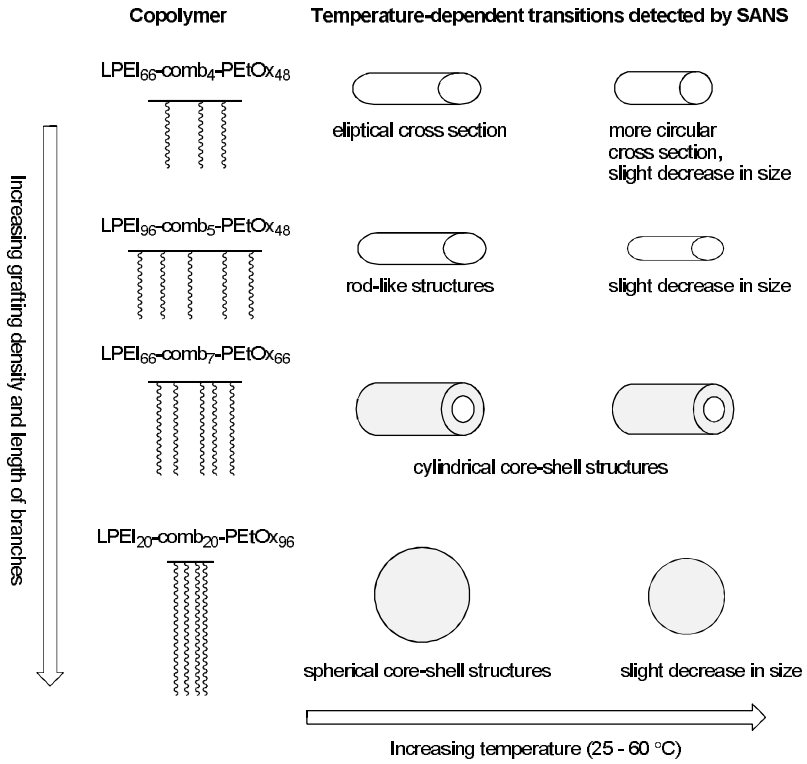

Figure 9. Shape transitions of LPEI-comb-PEtOx small particles with temperature and polymer composition. The objects are not drawn to scale.

Associated content

Supporting Information: Polymer characterization data and SANS analysis data. This information is available free of charge via the Internet at http://pubs.acs.org

Author Information

Corresponding author: * Tel: +44 (0)1865 275455; Fax: +44 (0)1865 275410;

E-mail: silviya.halacheva@chem.ox.ac.uk

Acknowledgments

We are grateful to EPSRC for financial support (EP/E029914/1). The SANS study was supported by the European Commission under the 6th Framework Programme through the Key Action: Strengthening the European Research Area, Research Infrastructures (Contract RII3-CT-2003-505925, Grant agreement N 226507-NMI3).

We thank Dr. Jean van den Elsen from the Department of Biology and Biochemistry at the University of Bath for access to the DLS instrument. We thank Prof. Stanislav Rangelov from the Institute of Polymers, Bulgarian Academy of Sciences for helpful discussions.

References

(1) Bajpai, A. K.; Shukla, S. K.; Bhanu, S.; Kankane, S. *Prog. Polym. Sci.* **2008**, *33*, 1088.

(2) Dimitrov, I.; Tzebicka, B.; Muller, A. H. E.; Dworak, A.; Tsvetanov, C. B. *Prog. Polym. Sci.* **2007**, *32*, 1275.

(3) Lowe, A. B.; McCormick, C. L. *ACS Symposium Series 780; ACS: Washington, DC,* **2001**, 1.

(4) Onaca, O.; Enea, R.; Hughes, D. W.; Meier, W. *Macromol.Biosci.* **2009**, *9*, 129.

(5) Forster, S.; Antonietti, M. *Adv. Mat.* **1998**, *10*, 195.

(6) Gebhart, C. L.; Kabanov, A. V. *J. Bioact. Biocompat. Polym.* **2003**, *18*, 147.

(7) Oerlemans, C.; Bult, W.; Bos, M.; Storm, G.; Frank, J.; Nijsen, W.; Hennik, W. E. *Pharm. Res*. **2010**, 2569.

(8) Schmaljohann, D. *Adv. Drug Deliv. Rev*. **2006**, *58*, 1655.

(9) Torchilin, V. P. *Pharm. Res.* **2007**, *24*, 1.

(10) Yokoyama, M. *Drug Discovery Today* **2002**, *7*, 426.

(11) Blanazs, A.; Armes, S. P.; Ryan, A. J. *Macromol. Rapid Commun.* **2009**, *30*, 267.

(12) Borisov, O. V.; Zhulina, E. B. *Macromolecules* **2003**, *36*, 10029.

(13) Borisov, O. V.; Zhulina, E. B. *Macromolecules* **2005**, *38*, 2506.

(14) Kosovan, P.; J. Kuldova; Limpouchova, Z.; Prochazka, K.; E.B. Zhulina; Borisov, O. V. *Macromolecules* **2009**, *42*, 6748.

(15) Li, Y.; Ghoreishi, S. M.; Warr, J.; Bloor, D. M.; Penfold, J.; Holzwarth, J. F.; Wyn-Jones, E. *Langmuir* **2001**, *17*, 5657.

(16) Smits, R. G.; Koper, G. J. M.; Mandel, M. *J. Phys.Chem.* **1993**, *97*, 5745.

(17) Koper, G. J. M.; van Duijvenbode, R. C.; Stam, D. D. P. W.; Steuerle, U.; Borkovec, M. *Macromolecules* **2003**, *36*, 2500.

(18) Aoi, K.; Okada, M. *Prog. Polym. Sci.* **1996**, *21*, 151.

(19) Kobayashi, S.; Uyama, H. *J. Poly. Sci.Part A* **2002**, *40*, 192.

(20) Jeong, J. H.; Song, S. H.; Lim, D. W.; Lee, H.; Park, T. G. *J. Control. Release* **2001**, *73*, 391.

(21) Kem, K. M. *J. Polym. Sci., Part A: Polym. Chem.* **1979**, *17*, 1977.

(22) Lambermount-Thijs, H. M.; van der Woerdt, F. S.; Baumgaertel, A.; Bonami, L.; Du Prez, F. E.; Schubert, U. S.; Hoogenboom, R. *Macromolecules* **2010**, *43*, 927.

(23) Tanaka, R.; Ueoka, I.; Takaki, Y.; Kataoka, K.; Saito, S. *Macromolecules* **1983**, *16*, 849.

(24) Saegusa, T.; Ikeda, H.; Fujii, H. *Macromolecules* **1972**, *5*, 108.

(25) Chatani, Y.; Kobatake, T.; Tadokoro, H. *Macromolecules* **1983**, *16*, 199.

(26) Chatani, Y.; Kobatake, T.; Tadokoro, H.; Tanaka, R. *Macromolecules* **1982**, *15*, 170.

(27) Chatani, Y.; Tadokoro, H.; Saegusa, T.; Ikeda, H. *Macromolecules* **1981**, *14*, 315.

(28) Hashida, T.; Tashiro, K.; Aoshima, S.; Inaki, Y. *Macromolecules* **2002**, *35*, 4330.

(29) Kakuda, H.; Okada, T.; Otsuta, M.; Katsumoto, Y.; Hasegawa, T. *Anal. Bioanal. Chem.* **2009**, *393*, 367.

(30) Kakuda, H.; Okada, M.; Hasegawa, T. *J. Phys.Chem. B* **2009**, 13910.

(31) Griffiths, P. C.; Alexander, C.; Nilmini, R.; Pennadam, S. S.; King, S. M.; Heenan, R. K. *Biomacromolecules* **2008**, *9*, 1170.

(32) Hsiue, G. H.; Chiang, H. Z.; Wang, C. H.; Juang, T. M. *Bioconjugate Chem.* **2006**, *17*, 781.

(33) Petersen, A.; Fechner, P. M.; Martin, A. L.; Kunath, K.; Stolnik, S.; Roberts, C. J.; Fischer, D.; Davies, M. C.; Kissel, T. *Bioconjugate Chem.* **2002**, *13*, 845.

(34) Wang, H.; Chen, X.; Pan, C. *J. Colloid Interface Sci.* **2008**, *320*, 62.

(35) Zhong, Z.; FeijenMartin, J.; Lok, C.; HenninkLane, V. C.; Yockman, J. W.; Kim, Y. H.; Kim, A. W. *Bioacromolecules* **2005**, *6*, 3440.

(36) Hoogenboom, R. *Angew. Chem. Int. Ed.* **2009**, *48*, 7978.

(37) Adams, N.; Schuber, U. S. *Adv. Drug Deliv. Rev.* **2007**, *59*, 1504.

(38) Christova, D.; Velichkova, R.; Loos, W.; Goethal, E. J.; Du Prez, F. *Polymer* **2003**, *44*, 2255.

(39) Hoogenboom, R.; Thijs, H. M. L.; Jochems, M. J. H. C.; van Lankvelt, B. M.; Fijten, M. W. M.; Schuber, U. S. *Chem. Commun*. **2008**, 5758.

(40) Weber, C.; Becer, C. R.; Hoogenboom, R.; Schuber, U. S. *Macromolecules* **2009**, *42*, 2965.

(41) Tomalia, D. A.; Hedstrand, D. M.; Feritto, M. S. *Macromolecules* **1991**, *24*, 1435.

(42) Hedstrand, D. M.; Tomalia, D. A.; Yin, R. *US Pat. No. WO/1996/022321* **1996**.

(43) Stuhrmann, H. B.; Burkhardt, N.; Dietrich, G.; Junemann, R.; Meerwinck, W.; Scmitt, M.; Wadzak, J.; Willumeit, R.; Zhao, J.; Nierhaus, K. H. *Nucl. Instrum. Methods* **1995**, *A356*, 133.

(44) Pedersen, J. S.; Posselt, D.; Mortensen, K. *J. Appl. Crystallogr.* **1990**, *23*, 321.

(45) Aoi, K.; Takasu, A.; Okada, M. *Macromol.Chem. Phys.* **1994**, *195*, 3835.

(46) Stawski, D.; Halacheva, S.; Bellmann, S.; Simon, F.; Polowinski, S.; Price, G. *J. Adhesion Sci. Technology* **2011**, *25*, 1481.

(47) Brissault, B.; Kichler, A.; Guis, C.; Leborgne, C.; Danos, O.; Cheradame, H. *Bioconjugate Chem.* **2003**, *14*, 581.

(48) Halperin, A.; Zhulina, E. B. *Europhys.Lett.* **1991**, *15*, 417.

(49) Dobrynin, A. V.; Rubinstein, M.; Obukhov, S. P. *Macromolecules* **1996**, *29*, 2974.

(50) Kokufuta, E.; Suzuki, H.; Yoshida, R.; Yamada, K.; Hirata, M.; Kaneko, F. *Langmuir* **1998**, *14*, 788.

(51) Halacheva, S.; Rangelov, S.; Haramus, V. M. *Macromolecules* **2007**, *40*, 8015.

(52) Rangelov, S.; Almgren, M.; Halacheva, S.; Tsvetanov, C. *J. Phys.Chem. C* **2007**, *111*, 13185.

(53) Schild, H. G. *Prog. Polym. Sci.* **1992**, *17*, 163.

(54) Chen, S. C.; Wilson, J.; Chen, W.; Davis, R. M.; Riffle, J. S. *Polymer* **1994**, *35*, 3587.

(55) Wu, G.; Chen, S. C.; Zhan, Q.; Wang, Y. Z. *Macromolecules* **2011**, *44*, 999.

(56) Glatter, O. *J. Appl. Crystallogr.* **1977**, *10*, 415.

(57) Hansen, S.; Pedersen, J. S. *J. Appl. Crystallogr.* **1991**, *24*, 541.

(58) Almgren, M.; Garamus, V. M.; Asakawa, T.; Jiang N. *J. Phys. Chem. B* **2007**, *111*, 7133.

(59) Rangelov, S.; Halacheva, S.; Garamus, V. M.; Almgren, M. *Macromolecules* **2008**, *41*, 8885.

For Table of Contents use only

The effects of temperature and polymer composition upon the aqueous solution properties of comb-like linear poly(ethylene imine)/poly(2-ethyl-2-oxazoline) based polymers

Silvia Halacheva, Gareth J. Price and Vasil M. Garamus